Journal of NUCLEAR SCIENCE and TECHNOLOGY, Vol. 42, No. 7, p. 626–635 (July 2005)

ORIGINAL PAPER

Systematics of Hydrolysis Constants of Tetravalent Actinide Ions

Hirotake MORIYAMA*, Takayuki SASAKI, Taishi KOBAYASHI and Ikuji TAKAGI

Department of Nuclear Engineering, Kyoto University, Yoshida, Sakyo-ku, Kyoto 606-8501

(Received February 17, 2005 and accepted in revised form April 20, 2005)

Systematic trends of mononuclear and polynuclear hydrolysis constants of tetravalent actinide ions were analyzed by using an electrostatic hard sphere model. The effective charges of actinide ions were introduced into the model by considering possible contributions of non-electrostatic interactions of actinide ions in addition to those of ordinary electrostatic ones. The systematic trends of hydrolysis constants were well fitted by the present model, and the parameter values such as the effective charges of actinide ions were determined. Some predictions were made and discussed in comparison with the solubility curves of tetravalent actinides.

KEYWORDS: hydrolysis constants, solubility, tetravalent actinide ions, hard sphere model

I. Introduction

The stability of hydrolysis and complex species has been discussed in many literatures in terms of the charge and ionic radius of the central metal ion.[1–7] Among those, the unified theory of metal ion complex formation constants which has been proposed by Brown and Sylva is one of the most successful models considering the effects of cations upon their anionic neighbours.[7] The model considers the electronic structure of the metal ion as well as the charge and ionic radius, and is used to predict stability constants for a large number of aqueous species composed of metal ions and ligands which are important for the safety assessment of radioactive waste disposal.[8] However, this model tends to give poorer estimates for higher coordination species, and requires some improvements.

In their approach, Neck and Kim have considered an energy term describing the inner-ligand electrostatic repulsion.[9] In this case, semi-empirical parameters are required to describe the effective electrostatic shielding between complexing ligand ions with the metal ion and hydration water molecules between them. By taking the parameter values determined from the selected formation constants, they have obtained excellent agreement between the calculated and experimental values even for higher coordination number. However, any further discussion has not been made for the systematic trends of actinide ions, for example, for the large differences between the hydrolysis constants of Th(IV) and those of other tetravalent actinides.[10]

In our approach, we have proposed a simple hard sphere model to describe the systematic trends in the hydrolysis behavior of actinide ions.[11,12] Reasonable agreement for higher coordination number has been obtained by taking into account the repulsive forces of hard spheres. Also, the effective charges of actinide ions have been introduced into the model by considering possible contributions of non-electrostatic interactions of actinide ions in addition to those of ordinary electrostatic ones, and systematic trends of the hydrolysis constants have been discussed by considering the additional interactions of 5f-orbitals.[12] Then, our model was extended to the polymeric hydrolysis constants of actinyl ions in our recent study.[13] It was found that, similarly to the case of monomeric hydrolysis species, the hydrolysis constants of polymeric species were well explained by the simple hard sphere model in which the effective charges of actinyl ions were introduced.

The present study is an extension of our previous one to the mononuclear and polynuclear hydrolysis constants of tetravalent actinide ions. In spite of extensive studies, the reliability of the hydrolysis constants of tetravalent actinide ions is still poor because of experimental difficulties such as very low solubility and colloid formation. For improvement, in our procedure, the reference values are carefully selected from the literatures and the systematic trends observed in the selected reference values are analyzed by the hard sphere model, in which not the formal but the effective charges of actinide ions are considered. Also some predictions are made and discussed in comparison with the solubility curves of tetravalent actinides.

II. Analytical Procedure

1. Selected Hydrolysis Constants

Because of the increasing needs for the reliable values in the safety assessment of radioactive waste disposal, a critical and comprehensive review of the available literatures has recently been performed for some of actinide elements in the NEA Thermochemical Data Base project.[14] In the case of tetravalent actinide ions, however, there are some sources of error, resulting in poor reliability. It should be kept in mind that the values of tetravalent actinide ions are often affected by colloid formation. As demonstrated by Knopp *et al.*,[15] for example, the formation of Pu(IV) colloids, which remain in solution without precipitation, is the predominant reaction when the concentration exceeds the solubility limit. This colloid formation may have led to misinterpretation of the experimental data. Also another source of error may arise from the formation of polynuclear species as suggested for Th(IV).[16]

In order to exclude such sources of error, in the present study, the $\beta_{1,1}$, $\beta_{1,2}$ and $\beta_{1,3}$ values of Th(IV)[17] and

*Corresponding author, Tel. +81-75-753-5824, Fax. +81-75-753-5824, E-mail: moriyama@nucleng.kyoto-u.ac.jp

Table 1 Selected hydrolysis constants of An(IV) ions

Species	Hydrolysis constant	Evaluated by NEA-TDB[14)]	Selected	Refs.	Calculated
Th(IV)	$\log \beta^{\circ}_{1,1}$	—	11.9±0.2	17)	12.20
	$\log \beta^{\circ}_{1,2}$	—	21.4±0.2	17)	21.60
	$\log \beta^{\circ}_{1,3}$	—	30.6	17)	30.37
	$\log \beta^{\circ}_{1,4}$	—	—		36.33
	$\log \beta^{\circ}_{1,5}$	—	—		36.90
	$\log \beta^{\circ}_{1,6}$	—	—		34.65
U(IV)	$\log \beta^{\circ}_{1,1}$	13.46±0.06	13.71±0.31	18)	14.33
	$\log \beta^{\circ}_{1,2}$	—	26.12±0.21	18)	25.80
	$\log \beta^{\circ}_{1,3}$	—	36.85±0.36	18)	36.64
	$\log \beta^{\circ}_{1,4}$	46.00±1.40	—		44.63
	$\log \beta^{\circ}_{1,5}$	—	47	10)	47.13
	$\log \beta^{\circ}_{1,6}$	—	—		46.77
Np(IV)	$\log \beta^{\circ}_{1,1}$	14.55±0.20	—		14.45
	$\log \beta^{\circ}_{1,2}$	28.35±0.30	—		26.02
	$\log \beta^{\circ}_{1,3}$	—	—		36.95
	$\log \beta^{\circ}_{1,4}$	47.70±1.10	—		45.00
	$\log \beta^{\circ}_{1,5}$	—	—		47.52
	$\log \beta^{\circ}_{1,6}$	—	—		47.16
Pu(IV)	$\log \beta^{\circ}_{1,1}$	14.60±0.20	—		14.51
	$\log \beta^{\circ}_{1,2}$	28.60±0.30	—		26.13
	$\log \beta^{\circ}_{1,3}$	39.70±0.40	—		37.10
	$\log \beta^{\circ}_{1,4}$	47.50±0.50	—		45.19
	$\log \beta^{\circ}_{1,5}$	—	—		47.72
	$\log \beta^{\circ}_{1,6}$	—	—		47.35

U(IV)[18)] are selected, which have been obtained by solvent extraction method with considerably low solute concentrations. Although the $\beta_{1,5}$ and $\beta_{1,6}$ values of U(IV)[19)] have been obtained by the solubility measurement with relatively low solute concentration up to 10^{-5} M, these values are not selected by considering possible colloid formation. Then the $\beta_{1,5}$ value of $<10^{47}$, which has been suggested by Neck and Kim[10)] to be consistent with the experimental data in neutral and alkaline solutions, is selected. As for Np(IV) and Pu(IV), the stepwise hydrolysis constants have been obtained by the solvent extraction studies using ^{239}Np and ^{238}Pu trace concentrations at I=1.0 M ($HClO_4/LiClO_4$).[20,21)] In their studies, however, it has not been confirmed that the results are free from any effects of possible coexistence of Np(V) and Pu(III). Thus no data are selected for Np(IV) and Pu(IV). It is important to note that the $\beta_{1,4}$ values of Th(IV) and U(IV) are not selected considering possible effect of colloid formation. **Table 1** shows the selected reference values for standard state hydrolysis constants, $\beta^{\circ}_{p,q}$, of actinide ions for the analysis of their systematic trends by the present model.

2. Hard Sphere Model

Similarly to the case of previous study,[12)] the improved hard sphere model is used in which the effective charges of central actinide ions are introduced. In the present study, however, a cubic structure of eight-coordination, which is different from the octahedral coordination in the previous study,[12)] is taken by considering a polymerization process for tetravalent actinide ion as given below. The central actinide ion and its ligands of water molecules and hydroxide ions are all treated as single hard spheres, and eight corners of the cubic structure are occupied by water molecules and/or hydroxide ions to form the hydrolysis species. For the formation of polymeric hydrolysis species of actinide ions, a polymerization process is assumed by considering the formation of the polymers bridged by hydroxide ions as shown in **Fig. 1**. Thomas was one of the first to interpret the polymerization phenomena in such a way as a result of his work on the hydrolysis reactions of metal ions.[22)] According to him, some irreversible elimination of water molecules, which is accompanied by the formation of oxygen bridges, may occur under appropriate conditions of high temperature, prolonged aging and/or high pH. For simplicity, however, the formation of oxygen bridges is not taken into account in the present study.

By considering the Coulomb interactions between the hard spheres, the electrostatic potential energy $E_{p,q}$ of each species is given by

$$E_{p,q} = \sum_{i \neq j}^{N} (Z_i Z_j / \varepsilon d_{ij}), \tag{1}$$

where N denotes the total number of hard spheres in the (p, q) species, Z_i and Z_j the electric charges of hard spheres i and j, respectively, ε the dielectric constant, and d_{ij} the distance between hard spheres i and j. As a substitute for the dipole moment, water molecules are assumed to have an effective (or apparent) charge. Concerning with the effective charges of actinide ions, it is important to note that non-electrostatic interactions of actinide ions, which are mainly due to the $5f$ electron orbital, act on not all the hard spheres

Species	Hydrolysis species
(1,q)	
(2,q)	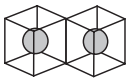
(3,q)	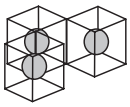
(4,q)	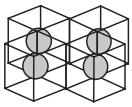
(5,q)	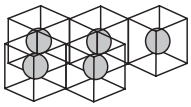
(6,q)	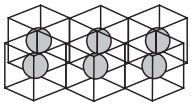
(7,q)	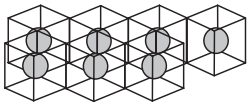
(p,q)	. . . . .

Fig. 1 Formation of polymeric hydrolysis species

but the first neighbors. Thus the effective charges of actinide ions are applied only for the first neighbors of water molecules and hydroxide ions while the formal charges are for the hard spheres other than the first neighbors. As for the dielectric constant, an improvement is introduced in the present model although a single constant has been assumed in the previous study.[12] In their electrostatic repulsion model, for example, Neck and Kim have used the geometry dependent dielectric constant by considering possible dependence of the electrostatic shielding on geometry. Such dependence may be due to different effects of water molecules in different geometries. Since all the effects of water molecules are included in the dielectric constant, in their model, it seems critically important to take the geometry dependent dielectric constant. In the present model, on the other hand, some of the neighboring water molecules are taken into account as hard spheres, and then much less effect may be expected due to the others. In order to minimize the number of free parameters, two types of the dielectric constant are used in the present study. One is the dielectric constant ε_1 for two ligands holding the central actinide ions between them. In this geometry, the electrostatic interaction between ligands is less affected by water molecules. The other denoted as ε_2 is for all other geometries in the coordination sphere.

By taking into account the coordinated water molecules, the mononuclear hydrolysis reaction for the $(1, q)$ species is given by

$$\mathrm{An(H_2O)_8}^{4+} + q\mathrm{OH}^- \rightleftarrows \mathrm{An(OH)}q\mathrm{(H_2O)_{8-}}_q{}^{4-q} + q\mathrm{H_2O}, \tag{2}$$

where each mononuclear species forms a cubic matrix in which an actinide ion is centered. For the polynuclear species, it is assumed to form connected cubes as shown in Fig. 1. In this structure, each actinide atom is in a cubic matrix connected to others by a double hydroxyl bridge –$(OH)_2$–, and the polymerization reactions for the (p, q) species with $p \geq 2$ are written as

$$p\mathrm{An(H_2O)_8}^{4+} + q\mathrm{OH}^- \rightleftarrows \mathrm{An}_p\mathrm{(OH)}_q\mathrm{(H_2O)_{8}}_{p-(3p-4)-q}{}^{4p-q} + (3p-4+q)\mathrm{H_2O}, \quad \text{for even } p \tag{3}$$

$$p\mathrm{An(H_2O)_8}^{4+} + q\mathrm{OH}^- \rightleftarrows \mathrm{An}_p\mathrm{(OH)}_q\mathrm{(H_2O)_{8}}_{p-(3p-5)-q}{}^{4p-q} + (3p-5+q)\mathrm{H_2O}, \quad \text{for odd } p. \tag{4}$$

Then, by combining reactions (2) to (4), the polymerization reactions for the (p, q) species can be generalized as

$$p\mathrm{An(H_2O)_8}^{4+} + q\mathrm{OH}^- \rightleftarrows \mathrm{An}_p\mathrm{(OH)}_q\mathrm{(H_2O)}_r{}^{4p-q} + (8p-r)\mathrm{H_2O}, \tag{5}$$

where $r=8-q$ for $p=1$ and $r=5p-q+[(-1)^{p-1}+9]/2$ for $p \geq 2$.

The potential energy change ΔE in reaction (5) is given by

$$\Delta E_{p,q} = E_{p,q} - pE_{1,0}, \tag{6}$$

where $E_{p,q}$ denotes the contribution of $\mathrm{An}_p\mathrm{(OH)}_q\mathrm{(H_2O)}_r{}^{4p-q}$ to the potential energy change and $E_{1,0}$ the contribution of $\mathrm{An(H_2O)_8}^{4+}$. In the present model, it is assumed that the free energy change of reaction (5) is mostly due to the potential energy change ΔE given by Eq. (6) and that all other contributions including hydration and entropy effects are compensated before and after reaction (5). In our previous study,[13] for example, the mononuclear and polynuclear hydrolysis constants of actinyl ions were well analyzed in this manner, and no apparent contribution other than the potential energy change ΔE given by Eq. (6) was observed. Thus, no other contribution is considered in the present study. Accordingly, the standard state hydrolysis constant $\beta^\circ_{p,q}$ of each species is expressed by

$$\beta^\circ_{p,q} = \exp(-\Delta E_{p,q}/RT), \tag{7}$$

where R and T denote the gas constant and absolute temperature, respectively.

III. Results

A least-squares fitting analysis of the selected $\beta^\circ_{p,q}$ values in Table 1 was carried out by using Eqs. (1), (6) and (7). In the analysis, the effective charges of Th^{4+} were assumed to

Table 2 Parameter values used and obtained in the analysis of hydrolysis constants

An(IV)	Th(IV)	U(IV)	Np(IV)	Pu(IV)
Z_{An}[a)]	4	4.42±0.05[b)]	4.42[c)]	4.42[c)]
Z_{OH}	−1	−1	−1	−1
Z_{H_2O}	−0.244±0.076[b)]	−0.244±0.076[b)]	−0.244[c)]	−0.244[c)]
r_{An} (nm)	0.108 [9,10]	0.104 [9,10]	0.102 [9,10]	0.101 [9,10]
r_{OH} (nm)	0.138 [21,22]	0.138 [21,22]	0.138 [21,22]	0.138 [21,22]
r_{H_2O} (nm)	0.138 [21,22]	0.138 [21,22]	0.138 [21,22]	0.138 [21,22]
ε_1[d)]	10.0±2.5[b)]	10.0±2.5[b)]	10.0[c)]	10.0[c)]
ε_2[d)]	16.6±4.1[b)]	16.6±4.1[b)]	16.6[c)]	16.6[c)]

[a)]Effective charges applied for the first neighbors of water molecules and hydroxide ions.
[b)]Standard errors.
[c)]Taken from the values determined for U(IV).
[d)]ε_1 is for ligands holding central actinide ion between themselves, and ε_2 for others.

be +4 without any contribution of non-electrostatic interactions, and the electric charge of OH^- was assumed to be −1. The ionic radii of actinide ions were taken from the literature values[9,10] as shown in **Table 2** and, for the lack of data, the ionic radius of 1.38×10^{-10} m[23,24] for O^{2-} was taken for H_2O. As well as the effective charge of U^{4+}, the other values of the effective charge and the dielectric constant of H_2O were treated as free parameters in the fitting analysis. The obtained results are summarized in **Tables** 2 and **3**, and the $\beta^\circ_{1,q}$ values obtained in the analysis are compared with the selected reference values in Table 1.

As shown in **Fig. 2**, the systematic behavior of the $\beta^\circ_{p,q}$ values is well described by the present model similarly to the case of monomeric species.[11,12] The $\beta^\circ_{p,q}$ values increase with the increasing number of hydroxide ions, but the extent of increase is not simply in proportion to the number due to the increasing repulsive interactions between the negatively charged ligand ions.

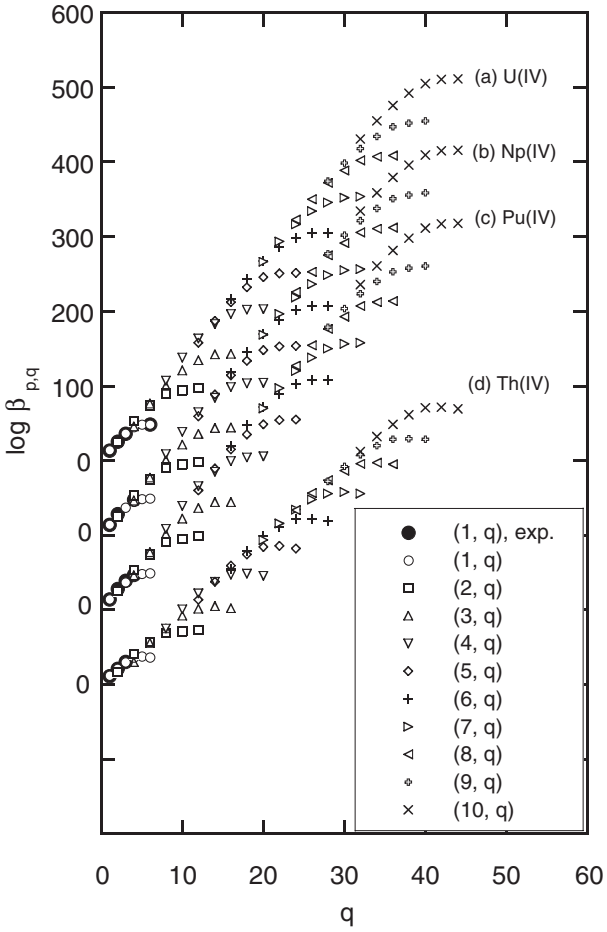

Fig. 2 $\log \beta^\circ_{p,q}$ values of An(IV) as a function of the q number; (a) U(IV), (b) Np(IV), (c) Pu(IV), (d) Th(IV)

IV. Discussion

1. Obtained Parameter Values

As shown in Table 2, the obtained effective charge of 4.42±0.05 for U^{4+} is larger than the formal charge of +4. The U^{4+} has not only the electrostatic interactions but also additional non-electrostatic interactions, similarly to the previous study.[12] Although the presently obtained value is a little larger than the value obtained in the previous study,[12] in which the effective charge of 4.368±0.145 has been determined for U^{4+}, this difference may be due to some differences between both studies. In fact, the cubic structure was assumed in the present study while the octahedral structure in the previous study. Also the ionic radii, which were obtained from the measured distances between atoms in solution species, were used in the present study while the ionic radii in crystals were used in the previous study. These differences in the selected structures and/or ionic radii are considered to result in some differences in the obtained parameter values. Similarly to the effective charge for U^{4+}, different values of the effective charge and the dielectric constant for H_2O were obtained, compared with the results of the previous study.[12] The effective charge of −0.244 for H_2O was obtained in the present study, which was less negative than the previous value of −0.57.[12] Also the dielectric constant was obtained to be 10.0 and 16.6 for the ligands holding the central actinide ions between them and for the others, respectively, which were larger than the previous value of 7.6.[12] It seems that the parameter values are much sensitive to the selected structures and/or ionic radii.

2. Predicted Hydrolysis Constants and Solubility Curves

As seen above, the parameter values of the present model

Table 3 Hydrolysis constants predicted in the present study

Species, (p, q)	$\log \beta^{\circ}_{p,q}$			
	Th(IV)	U(IV)	Np(IV)	Pu(IV)
1,1	12.20	14.33	14.45	14.51
1,2	21.60	25.80	26.02	26.13
1,3	30.37	36.64	36.95	37.10
1,4	36.33	44.63	45.00	45.19
1,5	36.89	47.13	47.52	47.72
1,6	34.65	46.77	47.16	47.35
2,2	18.05	26.04	26.26	26.37
2,4	41.42	53.65	54.10	54.32
2,6	56.82	73.16	73.77	74.08
2,8	67.70	88.06	88.80	89.17
2,10	68.90	91.21	91.97	92.36
2,12	68.88	93.12	93.89	94.29
3,4	32.65	48.59	48.99	49.20
3,6	58.05	78.26	78.91	79.24
3,8	76.18	100.54	101.37	101.80
3,10	91.20	119.65	120.65	121.15
3,12	98.73	131.16	132.25	132.80
3,14	99.85	136.14	137.27	137.85
3,16	93.48	133.51	134.63	135.19
4,8	76.98	109.04	109.95	110.41
4,10	102.28	138.61	139.77	140.35
4,12	122.54	163.06	164.42	165.11
4,14	136.24	180.83	182.34	183.10
4,16	144.26	192.83	194.44	195.25
4,18	142.91	195.31	196.94	197.76
4,20	137.17	193.32	194.93	195.75
5,12	116.70	160.97	162.31	162.99
5,14	140.07	188.58	190.15	190.95
5,16	159.17	211.84	213.60	214.49
5,18	172.36	229.10	231.01	231.97
5,20	179.04	239.73	241.73	242.74
5,22	177.35	241.87	243.89	244.91
5,24	170.52	238.78	240.77	241.77
6,16	157.18	217.52	219.33	220.25
6,18	179.19	243.74	245.77	246.80
6,20	197.50	266.20	268.42	269.54
6,22	208.64	281.37	283.72	284.90
6,24	215.74	292.44	294.87	296.11
6,26	214.01	294.53	296.99	298.23
6,28	207.50	291.77	294.20	295.43
7,20	196.01	268.54	270.77	271.91
7,22	216.86	293.58	296.02	297.26
7,24	232.95	313.78	316.40	317.72
7,26	243.81	328.68	331.42	332.80
7,28	248.81	337.61	340.42	341.85
7,30	247.68	340.30	343.14	344.57
7,32	241.39	337.76	340.58	342.00
8,24	234.72	323.29	325.98	327.34
8,26	255.89	348.65	351.56	353.03
8,28	271.43	368.30	371.37	372.92
8,30	281.18	382.06	385.24	386.85
8,32	288.27	393.11	396.39	398.05
8,34	286.12	394.78	398.07	399.74
8,36	280.19	392.59	395.87	397.52

Continued on the next page.

Continued.

Species, (p,q)	$\log \beta^{\circ}_{p,q}$			
	Th(IV)	U(IV)	Np(IV)	Pu(IV)
9,28	273.92	374.68	377.80	379.38
9,30	291.71	396.61	399.91	401.59
9,32	304.40	413.36	416.80	418.55
9,34	313.52	426.48	430.04	431.84
9,36	319.15	436.05	439.69	441.53
9,38	316.14	436.84	440.48	442.33
9,40	311.43	435.90	439.53	441.37
10,32	312.97	429.77	433.35	435.16
10,34	330.85	451.80	455.56	457.47
10,36	344.70	469.72	473.64	475.62
10,38	354.17	483.20	487.22	489.26
10,40	360.64	493.62	497.74	499.82
10,42	358.31	495.10	499.23	501.32
10,44	351.75	492.28	496.38	498.46

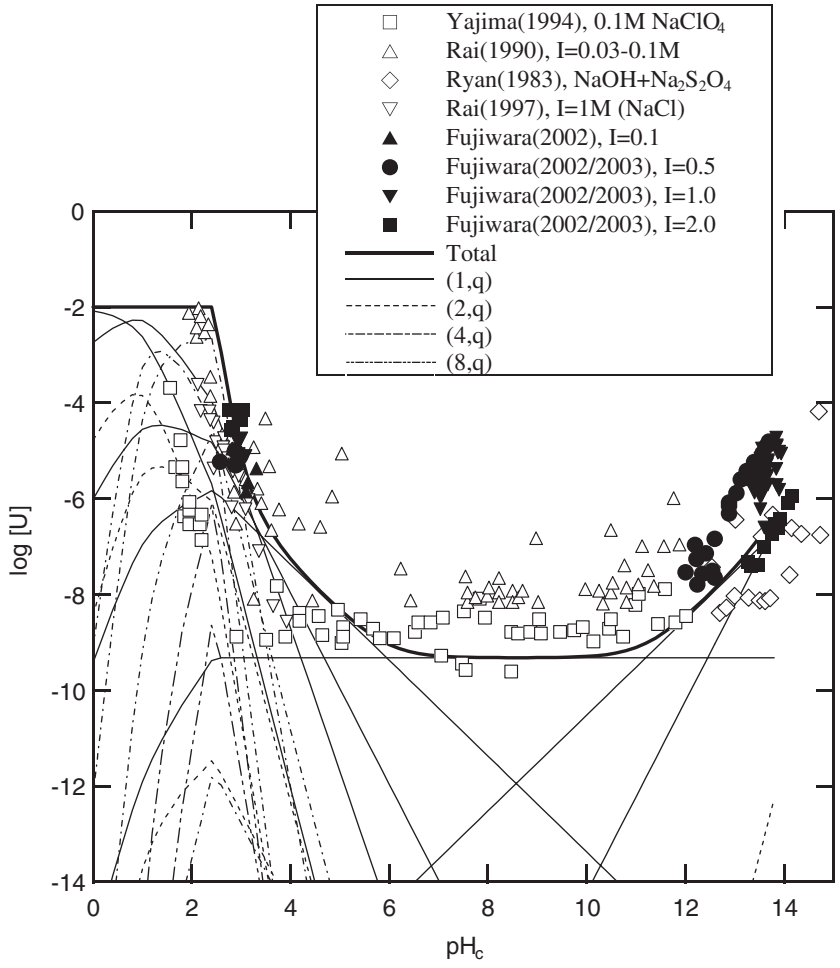

Fig. 3 Solubility and its component concentrations of U(IV) at 0.5 M $NaClO_4$ as a function of pH Bold curve denotes the total solubility including all the (p,q) species of $p \leq 10$.

is dependent on the selected structures and/or ionic radii. In spite of this constraint, however, it provides a basis not only to check abnormal experimental data but also to predict unknown values from a systematic point of view. For example, Fig. 2 shows the hydrolysis constant values predicted by the present model. It is interesting to compare such predicted values with some experimental results and to see what the consequence is.

Figure 3 shows a comparison of the predicted solubility curve with the experimental results of U(IV).[18,19,25–28] In

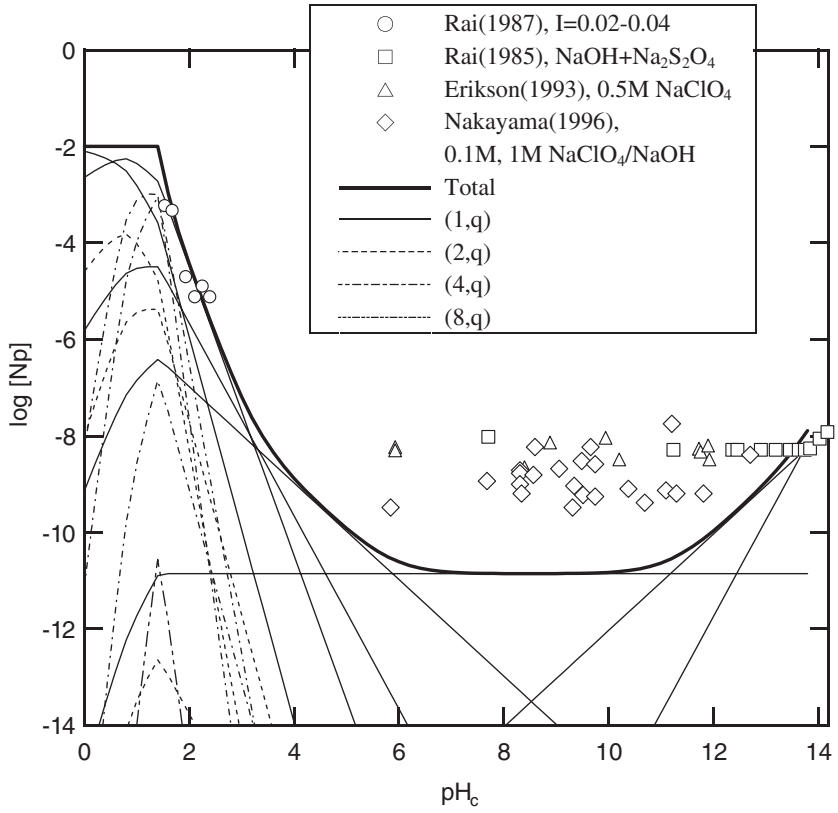

Fig. 4 Solubility and its component concentrations of Np(IV) at 0.5 M $NaClO_4$ as a function of pH Bold curve denotes the total solubility including all the (p, q) species of $p \leq 10$.

this case, the predicted solubility curve and its component concentrations are calculated with the hydrolysis constants, which are predicted by the present model and are corrected by the specific ion interaction theory (SIT).[14] The ion interaction parameter values of 0.76,[14] 0.54,[18] 0.52,[18] 0.23,[18] are taken for U^{4+}, UOH^{3+}, $U(OH)_2{}^{2+}$, $U(OH)_3{}^{+}$, respectively, and those for polynuclear species are temporarily assumed to be 0.76 for the species of ionic charges larger than +4 and 0 for anionic species. Also, the solubility limiting solid phase is assumed to be $UO_2 \cdot xH_2O$ with the solubility product value of $\log K_{sp}^{\circ} = -53.93$.[18] As shown in Fig. 3, the predicted solubility curve is consistent with the experimental results in the lower pH region. It is noticed, however, that there is a tendency in which the experimental solubility data are lying a little higher than the predicted solubility curve in near neutral and higher pH region. This may suggest possible contributions of colloid formation to the observed solubility data in this region. As predicted by the present model, the mononuclear and neutral species of $U(OH)_4{}^0$ are formed predominantly, which may aggregate easily to form colloids under usual physical interactions. Although such filtration techniques with very small pore sizes are applied to solubility measurements, it seems still difficult to remove all colloids of small sizes.

Figures 4 and **5** present similar comparisons of the predicted solubility curves with the experimental results of Np(IV)[29–32] and Pu(IV),[15,33–36] respectively. The predicted solubility curve and its component concentrations are calculated similarly to the above, by taking the same values of the ion interaction coefficients as those for U(IV) species and by taking the solubility product values for $NpO_2 \cdot xH_2O$ and $PuO_2 \cdot xH_2O$. The solubility product value of $\log K_{sp}^{\circ} = -57.97$[37] for $PuO_2 \cdot xH_2O$ is taken from our previous study and the value of $\log K_{sp}^{\circ} = -55.84$ for $NpO_2 \cdot xH_2O$ is estimated from those of $UO_2 \cdot xH_2O$ and $PuO_2 \cdot xH_2O$ by using a correlation suggested by Rai *et al.*[27] As shown in Figs. 4 and 5, the predicted solubility curves are again consistent with the experimental data in acidic region. Although the data of Perez-Bustamente[35] are much higher than the predited solubility, possible disproportionation of Pu(IV) has been pointed out by Rai.[33] Similarly to the above, it is also noticed that there are some contributions of colloid formation to the observed solubility data in near neutral and higher pH region.

Figure 6 shows a comparison of the predicted solubility curve with the experimental results of Th(IV).[38–40] The same values of the ion interaction coefficients as those for U(IV) species are taken for Th(IV) species, and the value of $\log K_{sp}^{\circ} = -47.41$ for $ThO_2 \cdot xH_2O$ is estimated from those of $UO_2 \cdot xH_2O$ and $PuO_2 \cdot xH_2O$ by using a correlation suggested by Rai *et al.*[27] In this case, it is interesting and important to note that most of the experimental solubility data other than those of Östhols *et al.*[40] are lying somewhat higher than the predicted solubility curve not only in near neutral and higher pH region but also in acidic region. Neck and Kim[10] have discussed the large discrepancies between the solubility products reported by different authors, and have suggested that the values are in reasonable agreement if

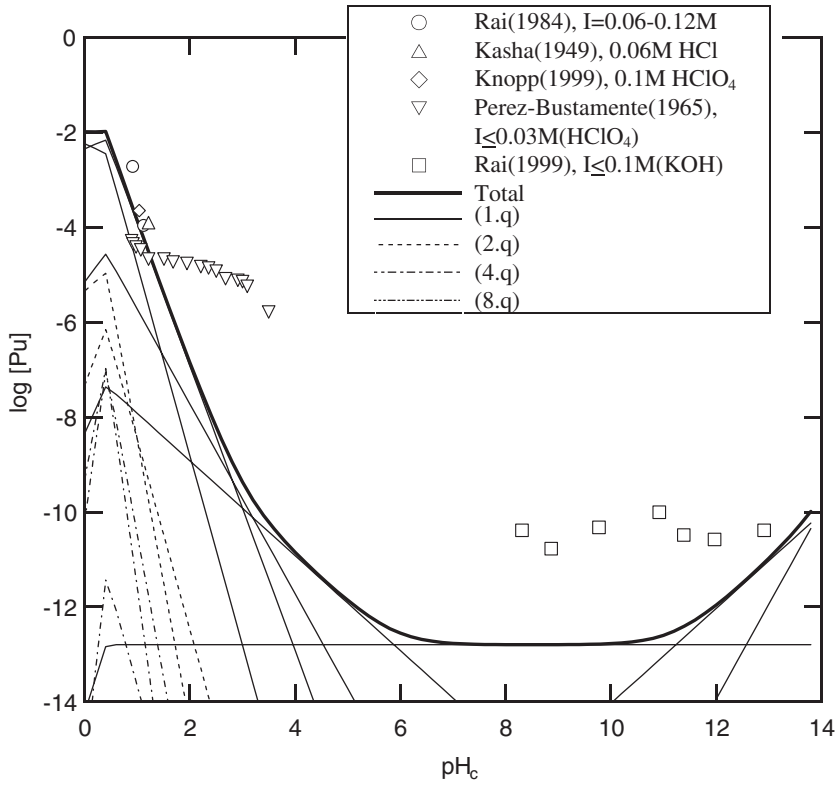

Fig. 5 Solubility and its component concentrations of Pu(IV) at 0.1 M $NaClO_4$ as a function of pH Bold curve denotes the total solubility including all the (p, q) species of $p \leq 10$.

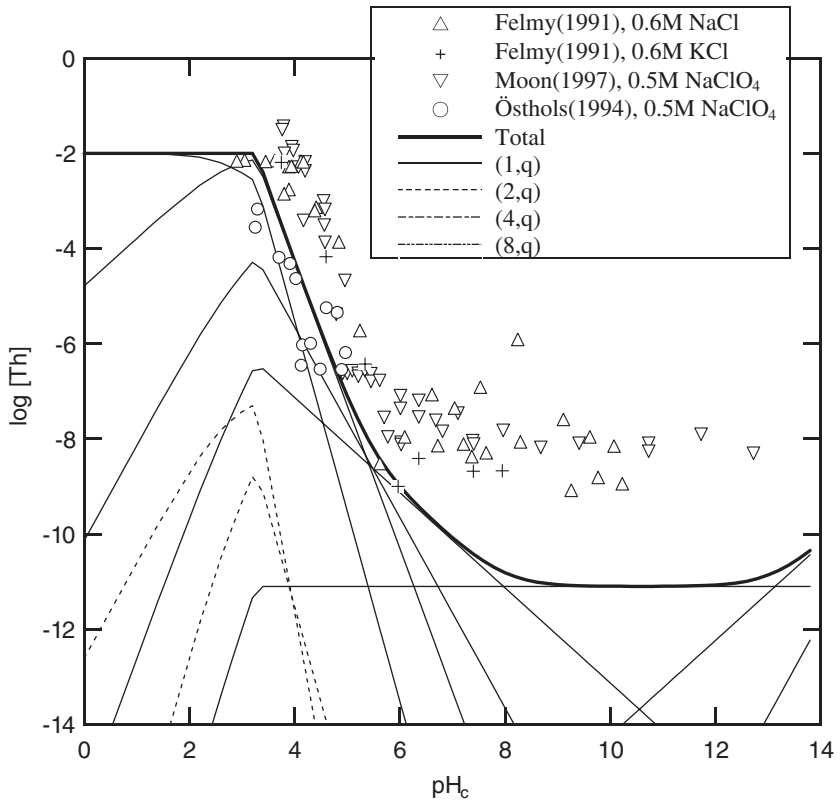

Fig. 6 Solubility and its component concentrations of Th(IV) at 0.5 M $NaClO_4$ as a function of pH Bold curve denotes the total solubility including all the (p, q) species of $p \leq 10$.

evaluated with their set of hydrolysis constants including the literature data for $Th_4(OH)_{12}^{4+}$ and $Th_6(OH)_{15}^{9+}$. In such a case, it is much important to confirm if the equilibrium is attained or not, since colloids are also present in solution and may affect the equilibrium. As shown in Fig. 6, the predicted solubility curve is rather close to the solubility data of Östhols *et al.*[40] for microcrystalline $ThO_2 \cdot xH_2O$, which represent a lower limit for an amorphous precipitate.

Some discrepancies between the experimental and predicted polynuclear hydrolysis constants are found for Th(IV) in the present study. As shown in Table 3, for example, the $\log \beta^{\circ}_{p,q}$ values for $Th_2(OH)_2^{6+}$, $Th_4(OH)_8^{8+}$ and $Th_4(OH)_{12}^{4+}$ are predicted to be 18.05, 76.98 and 122.54, respectively, while the experimental data have been reported to be 22.3, 91.6 and 141.3, respectively.[10] Although the observed discrepancies are so large, it may be noted that the formation of such polynuclear species is often assumed with little direct evidence. In fact, different species have often been suggested by different authors. Thus it is needed to obtain more direct evidence using various techniques. In this context, it is interesting to note that no predominant formation of polynuclear species of Th(IV) have been observed in a Th(IV) solution of 1×10^{-3} M in the study of Moulin *et al.* by using electrospray ionization mass spectrometry.[41]

V. Conclusions

The systematic trends of hydrolysis constants were well fitted by the present model, and the parameter values such as the effective charges of actinide ions were determined. Although the parameter values are dependent on the selected structures and/or ionic radii, the present model provides a basis not only to check abnormal experimental data but also to predict unknown values from a systematic point of view.

By using the hydrolysis constant values predicted by the present model, the solubility curves of tetravalent actinides were predicted and compared with the experimental ones. It was suggested that there are some contributions of colloid formation to the observed solubility data especially in near neutral and higher pH region. For the safety assessment of radioactive waste disposal, it is important to note that the lower solubility curves are predicted in this region.

References

1) C. W. Davies, "Electrolytic dissociation of metal hydroxide," *J. Chem. Soc.*, 1256 (1951).
2) H. Irving, R. J. P. Williams, "Stability of transition-metal complexes," *J. Chem. Soc.*, 3192 (1953).
3) R. J. P. Williams, "Stability of the complexes of the group IIA metal ions," *J. Chem. Soc.*, 3770 (1952).
4) C. F., Jr. Baes, R. E. Mesmer, *The Hydrolysis of Cations*, John Wiley and Sons, New York, (1976).
5) J. E. Huheey, *Inorganic Chemistry, 2nd ed.*, Harper and Row, New York, (1976).
6) I. Grenthe, I. Puigdommenech, *Modelling in Aquatic Chemistry*, OECD-NEA, Paris, (1997).
7) P. L. Brown, R. N. Sylva, "Unified theory of metal-ion-complex formation constants," *J. Chem. Res.*, (S)4-5, (M)0110 (1987).
8) P. L. Brown, H. Wanner, *Predicted Formation Constants Using the Unified Theory of Metal Ion Complexation*, OECD-NEA, Paris, (1987).
9) V. Neck, J. I. Kim, "An electrostatic approach for the prediction of actinide complexation constants with inorganic ligands-application to carbonate complexes," *Radiochim. Acta*, **88**, 815 (2000).
10) V. Neck, J. I. Kim, "Solubility and hydrolysis of tetravalent actinides," *Radiochim. Acta*, **89**, 1 (2001).
11) H. Moriyama, A. Kitamura, K. Fujiwara, H. Yamana, "Analysis of mononuclear hydrolysis constants of actinide ions by hard sphere model," *Radiochim. Acta*, **87**, 97 (1999).
12) H. Moriyama, K. Fujiwara, H. Yamana, "Systematics of complexation constants of actinide ions with inorganic ligands," *J. Nucl. Sci. Technol.*, Supplement **3**, 246 (2002).
13) H. Moriyama, T. Sasaki, T. Kobayashi, I. Takagi, "Systematics of polymeric hydrolysis constants of actinide ions," To be published in *J. Alloys Compounds*.
14) R. Guillaumont, Th. Fanghaenel, J. Fuger, I. Grenthe, V. Neck, D. A. Palmer, M. H. Rand, *Update on the Chemical Thermodynamics of Uranium, Neptunium, Plutonium, Americium and Technetium*, North-Holland, Amsterdam, (2003).
15) R. Knopp, V. Neck, J. I. Kim, "Solubility, hydrolysis and colloid formation of plutonium(IV)," *Radiochim. Acta*, **86**, 101 (1999).
16) I. Grenthe, B. Langmann, "Studies on metal carbonate equilibria. 23. Complex formation in the Th(IV)–H_2O–CO_2(g) system," *Acta Chem. Scand.*, **45**, 231 (1991).
17) C. Ekberg, Y. Albinsson, M. J. Comarmond, P. L. Brown, "Studies on the complexation behaviour of Thorium(IV); 1. Hydrolysis equilibria," *J. Solution Chem.*, **29**, 63 (2000).
18) K. Fujiwara, H. Yamana, T. Fujii, H. Moriyama, "Determination of uranium(IV) hydrolysis constants and solubility product of $UO_2 \cdot xH_2O$," *Radiochim. Acta*, **91**, 345 (2003).
19) K. Fujiwara, H. Yamana, T. Fujii, K. Kawamoto, T. Sasaki, H. Moriyama, "Solubility of uranium(IV) hydrous oxide in high pH solution under reducing condition," To be published in *Radiochim. Acta*.
20) J. Duplessis, R. Guillaumont, "Hydrolyse du Neptunium tetravalent," *Radiochem. Radioanal. Lett.*, **31**, 293 (1977).
21) H. Metivier, R. Guillaumont, "Hydrolyse du Plutonium tetravalent," *Radiochem. Radioanal. Lett.*, **10**, 27 (1972).
22) A. W. Thomas, T. H. Whitehead, "Ion interchanges in aluminum oxychloride hydrosols," *J. Phys. Chem.*, **35**, 27 (1931).
23) Y. Marcus, *Ion Solvation*, Wiley-Interscience, Chichester, (1985).
24) Y. Marcus, "Ionic radii in aqueous solutions," *Chem Rev.*, **88**, 1475 (1988).
25) T. Yajima, Y. Kawamura, S. Ueta, "Uranium(IV) solubility and hydrolysis constants under reduced conditions," *Mater. Res. Soc. Symp. Proc.*, **353**, 1137 (1994).
26) D. Rai, A. R. Felmy, J. L. Ryan, "Uranium(IV) hydrolysis constants and the solubility product of $UO_2 \cdot xH_2O$(am)," *Inorg. Chem.*, **29**, 260 (1990).
27) D. Rai, A. R. Felmy, S. M. Sterner, D. A. Moore, M. J. Mason, "The solubility of Th(IV) and U(IV) hydrous oxides in concentrated NaCl and $MgCl_2$ solutions," *Radiochim. Acta*, **79**, 239 (1997).
28) J. L. Ryan, D. Rai, "The solubility of uranium(IV) hydrous oxide in sodium hydroxide solutions under reducing conditions," *Polyhedron*, **2**, 947 (1983).
29) D. Rai, J. L. Swanson, J. L. Ryan, "Solubility of $NpO_2 \cdot xH_2O$(am) in the presence of Cu(I)/Cu(II) redox buffer," *Radiochim. Acta*, **42**, 35 (1987).

30) D. Rai, J. L. Ryan, "Neptunium(IV) hydrous oxide solubility under reducing and carbonate conditions," *Inorg. Chem.*, **24**, 247 (1985).
31) T. E. Erikson, P. Ndalamba, D. Cui, J. Bruno, M. Caceci, K. Spahiu, SKB Technical Report, TR 93-18, Stockholm, (1993).
32) S. Nakayama, T. Yamaguchi, K. Sekine, "Solubility of Np(IV) hydrous oxide in aqueous solutions," *Radiochim. Acta*, **74**, 15 (1996).
33) D. Rai, "Solubility product of Pu(IV) hydrous oxide and equilibrium constants of Pu(IV)/Pu(V), Pu(IV)/Pu(VI), Pu(V)/Pu(VI) couples," *Radiochem. Acta*, **35**, 97 (1984).
34) M. Kasha, *The Transuranium Elements*, Eds. G. T. Seaborg, J. J. Katz, W. M. Manning, Research Papers, McGraw-Hill, New York, p. 295 (1949).
35) J. A. Perez-Bustamente, "Solubility product of tetravalent plutonium hydroxide and study of the amphoteric character of hexavalent plutonium hydroxide," *Radiochim. Acta*, **4**, 67 (1965).
36) D. Rai, N. J. Hess, A. R. Felmy, D. A. Moore, M. Yui, P. Vitorge, "A thermodynamic model for the solubility of PuO_2(am) in the aqueous K^+–HCO_3^-–CO_3^{2-}–OH^-–H_2O system," *Radiochim. Acta*, **86**, 89 (1999).
37) K. Fujiwara, H. Yamana, T. Fujii, H. Moriyama, "Solubility product of plutonium hydrous oxide and its ionic strength dependence," *Radiochim. Acta*, **90**, 857 (2002).
38) H. Moon, *Equilibrium Ultrafiltration of Hydrolyzed Thorium(IV) Solutions*, Bull. Korean Chem. Soc., Vol. 10, p. 270 (1989).
39) A. R. Felmy, D. Rai, M. J. Mason, "The solubility of hydrous thorium(IV) oxide in chloride madia: Development of an aqueous ion-interaction model," *Radiochim. Acta*, **55**, 177 (1991).
40) E. Östhols, J. Bruno, I. Grenthe, "On the influence of carbonate on mineral dissolution; III. The solubility of microcrystalline ThO_2 in CO_2–H_2O Media," *Geochim. Cosmochim. Acta*, **58**, 613 (1994).
41) C. Moulin, B. Amekraz, S. Hubert, V. Moulin, "Study of thorium hydrolysis species by electrospray-ionization mass spectrometry," *Anal. Chim. Acta*, **441**, 269 (2001).